TriNet "ShakeMaps": Rapid Generation of Peak Ground Motion and Intensity Maps for Earthquakes in Southern California

David J. Wald, M.EERI, Vincent Quitoriano, Thomas H. Heaton, M.EERI, Hiroo Kanamori, M.EERI, Craig W. Scrivner, and C. Bruce Worden

Rapid (3-5 minutes) generation of maps of instrumental ground-motion and shaking intensity is accomplished through advances in real-time seismographic data acquisition combined with newly developed relationships between recorded ground-motion parameters and expected shaking intensity values. Estimation of shaking over the entire regional extent of southern California is obtained by the spatial interpolation of the measured ground motions with geologically based frequency and amplitude-dependent site corrections. Production of the maps is automatic, triggered by any significant earthquake in southern California. Maps are now made available within several minutes of the earthquake for public and scientific consumption via the World Wide Web; they will be made available with dedicated communications for emergency response agencies and critical users.

INTRODUCTION

The most common information available immediately following a damaging earthquake is its magnitude and epicentral location. However, the damage pattern is not a simple function of these two parameters alone, and more detailed information must be provided to properly ascertain the situation. For example, for the February 9, 1971 earthquake, the northern San Fernando Valley was the region with the most damage, even though it was more than 15 km from the epicenter. Likewise, areas strongly affected by the Loma Prieta and Northridge, California, earthquakes that were either distant from the epicentral region or out of the immediate media limelight were not fully appreciated until long after the initial reports of damage. Most recently, the full extent of damage from the 1995 Kobe, Japan, earthquake was not recognized by the central government in Tokyo until many hours later (e.g., Yamakawa, 1997), delaying rescue and recovery efforts.

(DJW) U.S. Geological Survey, 535 S. Wilson Ave., Pasadena, CA 91106
(VQ, THH, HK, CBW) Seismological Laboratory, Caltech, Pasadena, CA 91125
(CWS) Calif. Dept. of Conserv., Div. Mines and Geology, Sacramento, CA 95814

©*Earthquake Spectra*, Volume 15, No. 3, August 1999

As part of the research and development efforts of the TriNet (California Institute of Technology, the California Division of Mines and Geology, and the U. S. Geological Survey) project (see Mori et al., 1998), we have been creating "ShakeMap" for earthquakes (magnitude greater than 3.0) in southern California for the last two years (Wald et al., 1997). We currently generate separate maps of the spatial distribution of peak ground motions (acceleration, velocity, and spectral response) as well as a map of instrumentally derived seismic intensities. These maps provide a rapid portrayal of the extent of potentially damaging shaking following an earthquake and can be used for emergency response, loss estimation, and for public information through the media. For example, maps of shaking intensity can be combined with databases of inventories of buildings and lifelines to rapidly produce maps of estimated damage (e.g., Eguchi et al., 1997). Recent advances in loss estimation now allow for the direct use of recorded ground motion parameters (e.g., Kircher et al., 1997; NIBS, 1997) without using Modified Mercalli Intensity as an intermediate parameter. Generation of the maps is fully automatic, triggered by any significant earthquake in southern California and made available within several minutes of the earthquake for public and scientific consumption via the World-Wide-Web; they will be made available with more reliable, dedicated communications for emergency response agencies in the near future.

Such maps have traditionally been difficult to produce rapidly and reliably due to limitations of seismic network instrumentation and data telemetry. In addition, adequate relationships between recorded ground motions and damage intensities have only recently been developed (for example, the JMA seismic intensity scale, Japan Meteorological Agency, 1996). However, with recent advances in digital communication and computation, it is now technically feasible to develop systems to display ground motions in an informative manner almost instantly.

A detailed description of the shaking over the entire southern California region requires interpolation of the measured ground motions. In addition, simple geologically based, frequency and amplitude-dependent site correction factors, currently under development, provide a useful first-order correction for local amplification in areas that are not instrumented. In this report we present ongoing efforts addressing the issues pertinent to rapid ground-motion map making.

GENERATION OF INSTRUMENTAL GROUND MOTION MAPS

The current TriNet seismic station distribution in southern California is shown in Figure 1. Signals from the USGS-Caltech stations (triangles) are acquired in real time using a variety of digital telemetry methods (see Mori et al., 1998, for more details). The California Division of Mines and Geology, CDMG, stations (square) are near-real time, utilizing an automated telephone dial-up procedure (see Shakal et al., 1996, 1998). As of March, 1999, there were 80 USGS-Caltech real-time stations online and nearly 100 CDMG dialup stations; in all there will be approximately 670 TriNet strong-motion stations in the next three years. The generation of ShakeMaps is triggered automatically by the event associator of the Southern California Seismic Network (SCSN), operated by the USGS and Caltech. Within the first minute following the shaking, ground-motion parameters are available from the USGS-Caltech component of the network and within several minutes most of the important near-source CDMG stations contribute. A more complete CDMG contribution is available approximately within the first half hour. Initial maps are made

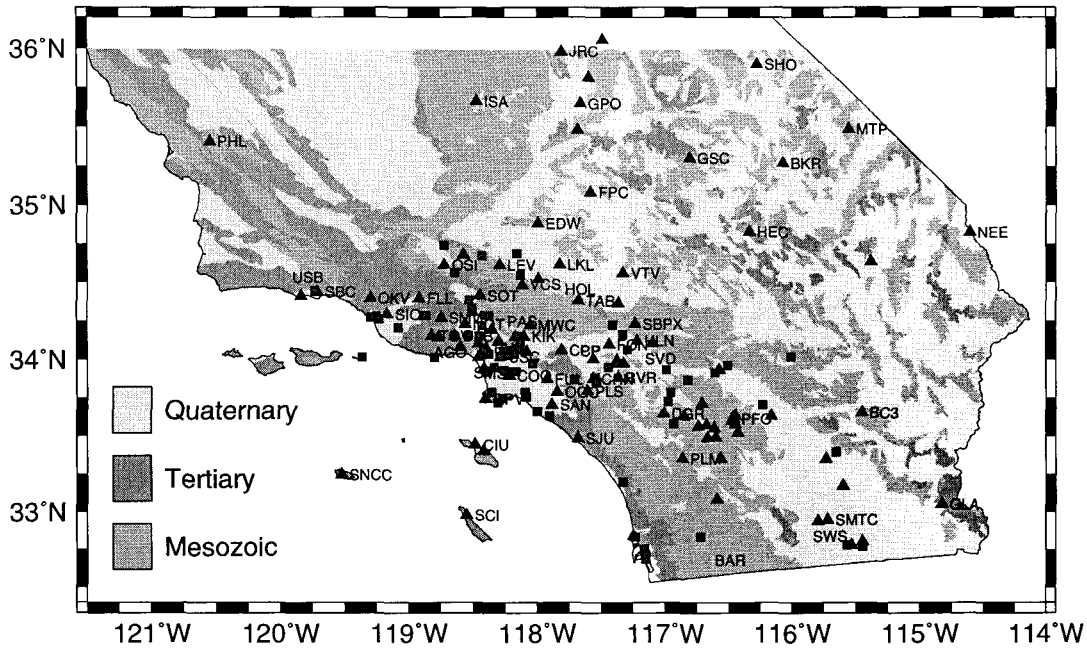

Figure 1. Map of southern California showing current TriNet station distribution. CDMG stations are shown as squares and USGS-Caltech stations are depicted with triangles. Shading indicates the Quaternary, Tertiary, and Mesozoic (QTM) geologic unit designations of Park and Ellrick (1998) as shown in the legend.

with just the real-time component of TriNet, but they are updated automatically as more data are acquired. Parametric data from the stations include peak ground acceleration (PGA), peak ground velocity (PGV), and peak response spectral amplitudes (at 0.3 sec, 1 sec, and 3 sec).

Shaking maps are prepared by contouring shaking information interpolated onto a square grid uniformly sampled at a spacing of 2.8-km (0.025°) throughout southern California. If there were stations at each of the 45,000 grid points, then the creation of shaking maps would be relatively simple. Of course stations are not available for all of these grid points, and in many cases grid points may be tens of kilometers from the nearest reporting station. The overall mapping philosophy is to combine information from individual stations, geology (representing site amplification), and the distance to the centroid to create the best composite map. The procedure should produce reasonable estimates at grid points located far from available data, while preserving the detailed shaking information available for regions where there are stations nearby.

ESTIMATED MOTIONS IN SPARSE AREAS

In Figure 2 we show an example of the processing steps for a peak acceleration map of the magnitude 4.4 earthquake near Wrightwood, California, (about 60 km northeast of Los Angeles) that occurred on August 20, 1998. First, peak ground motion parameters are recovered for each station and associated with a particular earthquake origin

time and epicenter (Figure 2a). In regions of sparse station spacing, ground motions are estimated using magnitude-distance regressions from the strong motion "centroid" (Kanamori, 1993). To determine the strong motion centroid, we apply empirically derived station corrections and then fit the observed ground motions to find the best equivalent point-source latitude, longitude, and magnitude (Kanamori, 1993). We scan the parameter space to determine the global minimum solution for location and magnitude, and then refine the solution using the method of least squares. The magnitude is M_L, and the station corrections are also calibrated to the Wood-Anderson instrument response (natural period of about 0.8 sec). These empirical station corrections are used only to compute the magnitude for estimating ground motions; they are not further used in the processing.

We create a coarse, uniformly spaced grid of 30-km spaced "phantom" stations. Peak ground motions are assigned to each coarse grid point using the Joyner and Boore (1981) distance attenuation relationship for "rock sites" and the magnitude of the centroid and its distance to each grid point. Peak response spectral values (0.3, 1.0, and 3.0 sec) are similarly estimated using Boore et al. (1994). However, as shown in Figure 2b, only those phantom stations further than 30 km from all TriNet stations are retained. Likewise, the peak values at the location of the centroid itself are only used if there are no nearby stations (<10 km). In Figure 2b, the epicenter is given by a filled star, the centroid is shown with an unfilled star, and the phantom stations at which ground motions are estimated are shown as circles. For this region, the TriNet station distribution is sufficiently dense that only 10 phantom stations are required on the scale of the map shown. All other predicted values in this case are superseded by recorded amplitudes. Out at greater distances, however, more phantom stations do contribute and they insure that the contour maps remain well-behaved and bounded at the edges.

SITE CORRECTIONS

Site corrections are used to interpolate from ground motions recorded on a fairly sparse, non-uniformly spaced network of stations to maps showing spatially continuous functions (i.e., contours). For example, direct interpolation between rock sites surrounding a basin would inadequately represent the true, amplified motion within the basin.

Prior to interpolation, we reduce the ground motion amplitudes to a common reference, in this case bedrock motions. Peak ground motion amplitudes from the TriNet stations are corrected to rock site conditions (using a procedure described later); and the observations (corrected to rock) and the coarse phantom stations (computed for rock) are then interpolated to a fine rock site grid (2.8-km spacing, see Figure 2c). Finally, the interpolated rock grid is corrected at each point for local site amplification. A continuous surface which is fit to the fine grid is then contoured (Figure 2d).

The finely interpolated grid has been predefined and so we can preassign a geologically based site classification to each location. Likewise, the station locations are associated with the QTM classification based on the QTM map, and not on independent geological classification at the station. The amplification correction we use is based on the Quaternary, Tertiary, Mesozoic ("QTM") geological classification of Park and Ellrick (1998). These categories can be considered to represent soil, soft rock, and hard rock, respectively, and hence they provide a very simple but effective way to assign amplification on a regional scale. The QTM map's northern extent is at 36° north latitude

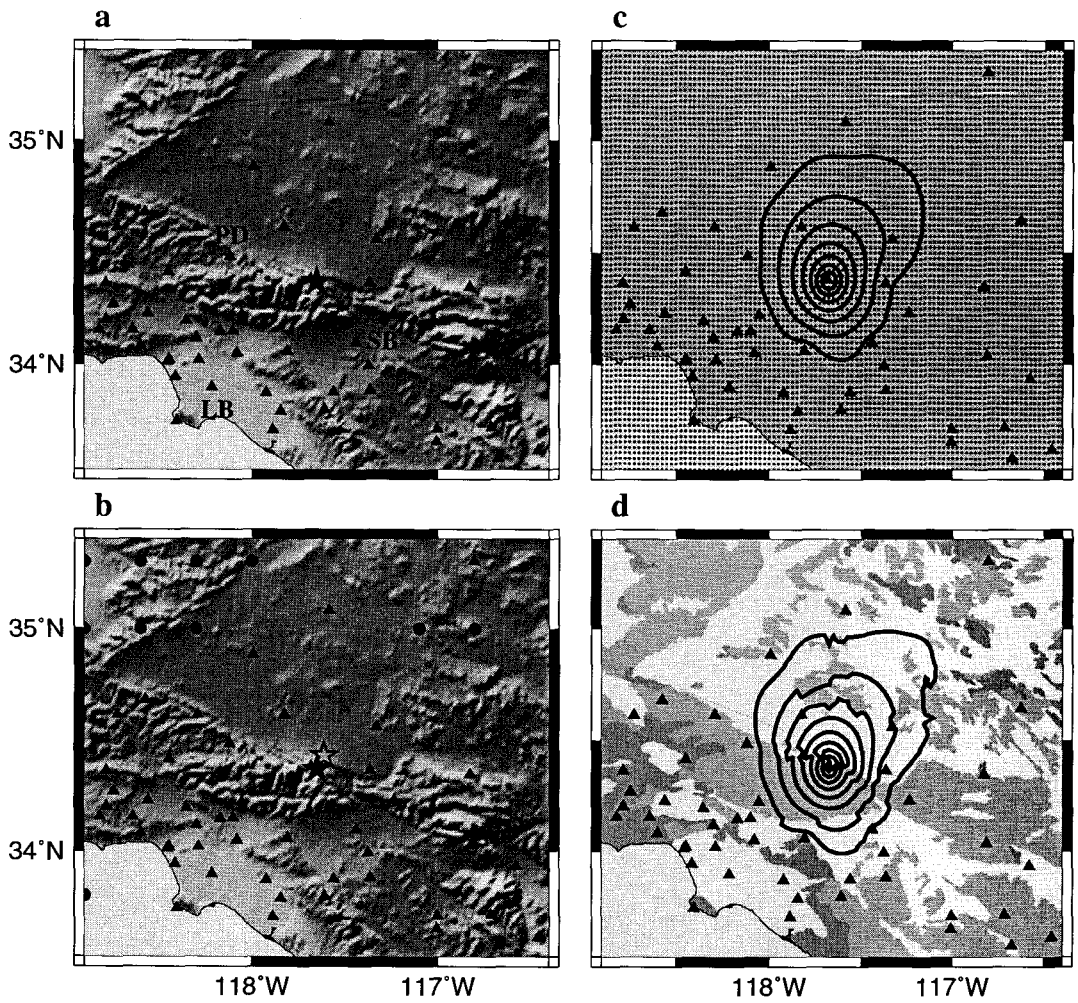

Figure 2. Steps in ShakeMap processing for the August 20, 1998 magnitude 4.4 Wrightwood earthquake. a) Shaded relief basemap showing epicenter (star) and recordings stations (triangles). SB, LB, and PD denote locations of the cities San Bernardino, Long Beach, and Palmdale, respectively. b) Same as a) but with the addition of the centroid (open star) and sites of estimated peak ground motions (circles). c) Finely spaced grid (2.8 km, circles) and contours of peak acceleration site-corrected to bedrock. d) Contours of site-corrected peak acceleration overlaid on the QTM geology basemap (see text and Figure 1 for more details).

and the southern boundary coincides with the U.S.A./Mexico border. However, we have continued the trend of the Imperial Valley and Peninsular Ranges south of the border by approximating the geology based on the topography; Mesozoic rock was assigned to sites above 100 meters in elevation and Quaternary soil was assigned to those below 100 meters. This results in continuity of our site correction across the international border.

Table 1. Site amplification factors

Period (sec)	Input Rock Peak Ground Acceleration			
	<15%g	15-25%g	25-35%g	>35%g
Mesozoic (589 m/sec):				
0.1-0.5	1.00	1.00	1.00	1.00
0.4-2.0	1.00	1.00	1.00	1.00
Tertiary (406 m/sec)				
0.1-0.5	1.14	1.10	1.04	0.98
0.4-2.0	1.27	1.25	1.22	1.18
Quaternary (333 m/sec)				
0.1-0.5	1.22	1.15	1.06	0.97
0.4-2.0	1.45	1.41	1.35	1.29

To obtain site amplification factors based on these QTM categories, we use the mean shear-wave velocities assigned to them (Park and Ellrick, 1998), and apply the frequency and amplitude-dependent amplification factors determined by Borcherdt (1994) based on these velocities. Given the mean 30-meter shear velocities shown in Table 1, the amplifications can be calculated for short-period (0.1-0.5 sec) and mid-period (0.4-2.0 sec) ranges from Borcherdt (1994) equations 7a and 7b, respectively, at four ranges of input acceleration levels (Borcherdt, 1994, Table 2). These amplification factors are given in Table 1. The amplification for the soil (Quaternary Alluvium) sites decreases with increasing ground motion levels; Tertiary and Mesozoic rock units have a less pronounced amplitude dependency (see Table 1).

We scale the PGA amplitude with the short-period amplification factors while the PGV values are corrected with the mid-period factors. Response spectral values are scaled by the short-period factors at 0.3 sec, and by the mid-period response at 1.0 and 3.0 seconds. The site correction procedure is applied so that the original data values are returned at each station; hence, the actual recorded motions are preserved in the process and the final contours reflect the observations wherever they exist.

Finally, we contour the interpolated, site-corrected PGA, PGV, and response spectral values. The interpolation and contouring is done using tools available with Generic Mapping Tools (GMT, Wessel and Smith, 1991). The contouring consists of finding an adjustable-tension (interior and boundary tension factor of 0.4), continuous-curvature surface that fits the constraining data exactly (Smith and Wessel, 1990). To summarize the map-making steps (corresponding to the letters in Figure 2), we:

a) Gather the observed peak ground motions at recording stations.

b) Determine the centroid (magnitude and location) and estimate ground motions on rock at sites far from recording stations.

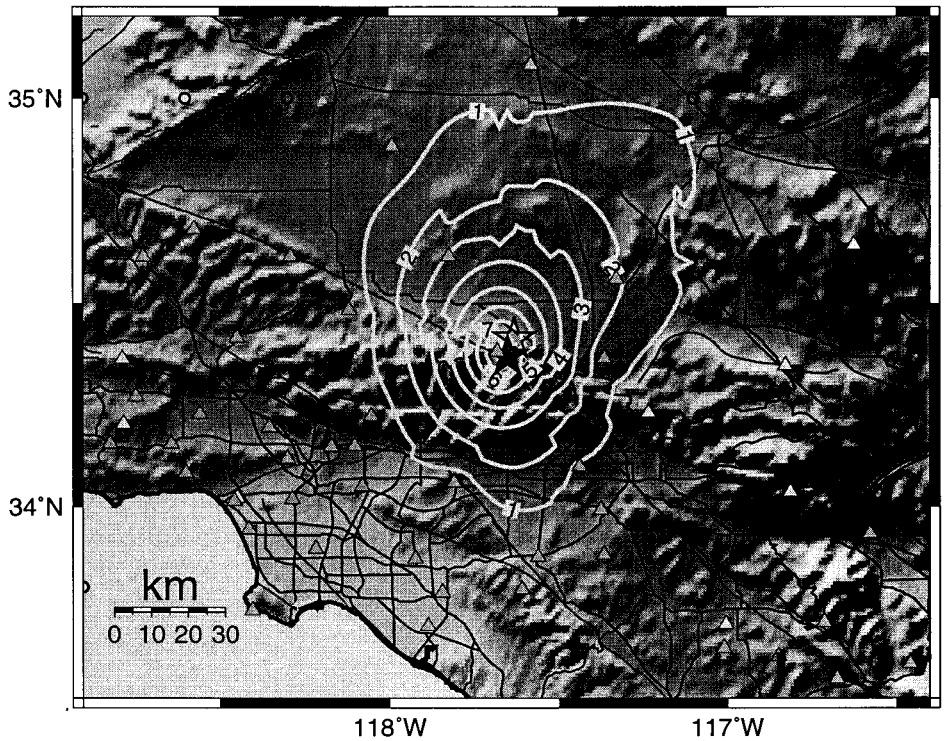

Figure 3. Shaded relief map showing peak accelerations for the August 20, 1998 magnitude 4.4 Wrightwood earthquake with contours of acceleration in percent "g." Triangles represent stations; dark lines are freeways and lightly shaded lines are mapped faults. The shaded star shows the epicenter and the open star represents the strong motion centroid. Open circles represent phantom grid stations (see text for details).

c) Correct the data to rock based on the site QTM geology and interpolate the data plus the predicted ground motions onto a fine (2.8 km) rock grid.

d) Site amplify at each fine grid point based on its site QTM geology and amplitude, fit a smooth function through all fine grid points, and contour.

The PGA ShakeMap associated with the example event is shown in Figure 3. Since site amplification factors are high at low levels of shaking, applying the site corrections to small earthquakes shows noticeable effects, especially when the observations alone are insufficient to show the amplification variations.

NORTHRIDGE EARTHQUAKE EXAMPLE

Although only relatively small events have been recorded in the two years since we began making "ShakeMap," we can apply the same processing procedure to data sets from larger past earthquakes. In Figure 4 we show a map of the recorded peak velocity distribution (contoured in cm/sec) for the 1994 magnitude 6.7 Northridge earthquake to illustrate the nature of the information generated by ShakeMap and the effects of applying the site correction for a larger earthquake. For Figure 4, we have not yet applied the

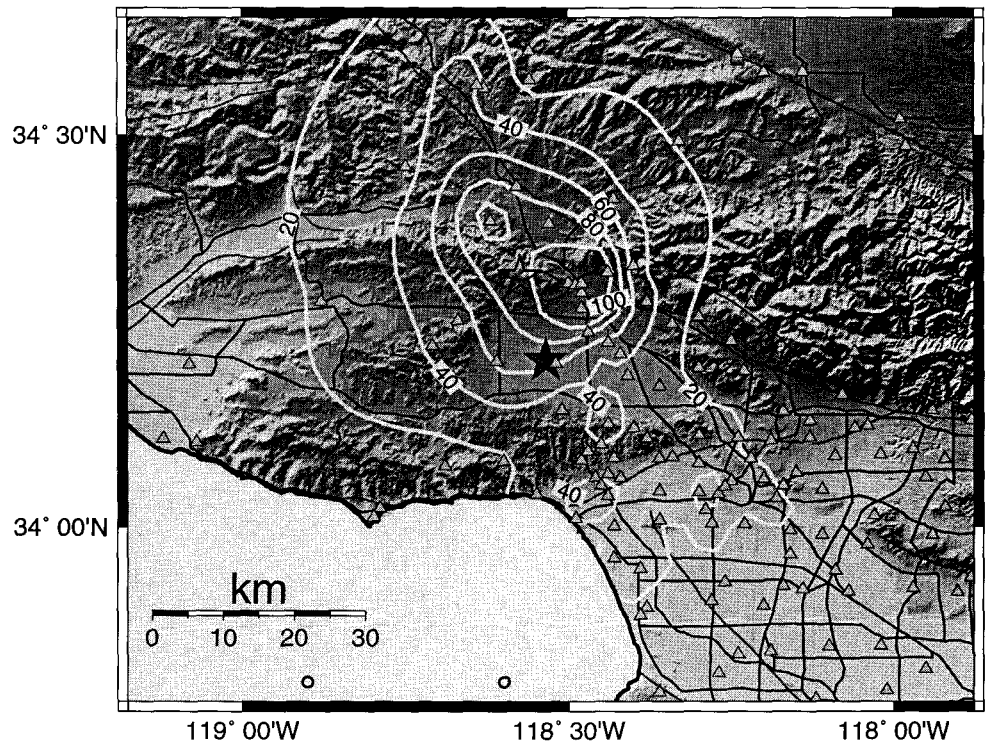

Figure 4. Shaded relief map showing recorded peak velocity contours for the magnitude 6.7 1994 Northridge earthquake. Contours of velocity are in cm/sec. The shaded star shows the epicenter, the open star represents the strong motion centroid, and open circles represent phantom grid stations. No site corrections have been applied.

site correction. The contour pattern is only a reflection of the motions as recorded (not corrected to bedrock); likewise, the effect of our gap-filling is negligible in this case since there are only two predicted phantom stations on the scale of this map (the two circles shown in the ocean). In this particular example, the ground-motion data are from existing analog networks (CDMG, USGS, University of Southern California, Southern California Edison, the Los Angeles Department of Water and Power), not the current TriNet digital instrument deployment, which postdates the Northridge earthquake.

Typically, for moderate-to-large events, the pattern of peak ground velocity reflects the pattern of the earthquake faulting geometry, with largest amplitudes in the near-source region, and in the direction of rupture directivity (Figure 4). For the Northridge earthquake, rupture updip and toward the north resulted in significant directivity in that direction. Differences between rock and soil sites are apparent, but the overall pattern is more a reflection of the source proximity and rupture process. While the site effects are still important (see the tabulated amplification factors in Table 1), we expect that site corrections for larger events (which are dominated by strong shaking) are less significant than for the lower shaking levels associated with smaller earthquakes. This is particularly true at higher frequencies.

The site-corrected peak velocity map for the Northridge earthquake is shown in Fig-

ure 5. The differences between the ground velocities within the valleys and surrounding mountains become more evident once the site corrections are applied. In addition, originally smooth contours that simply connected remote stations become more complex when intervening geologically based site corrections play a role in determining the interpolated amplitudes. For example, due to alluvium in the east-west trending Santa Clara River basin (SCB, Figure 5), the site correction increases the peak velocities with respect to the surrounding mountains.

Naturally, the site correction has a more dramatic effect where the station coverage is sparse. Where there are sufficient ground-motion data, the recorded amplitudes *define* the site effects, and nearby site corrections are applied with respect to these observations. In areas lacking observations, the amplitude pattern variations primarily reflect the site corrections modifying an otherwise smoothly varying function of amplitude. In this respect, for areas of sparse coverage, we can consider the application of the geology based site corrections to be adding data (in the form of our knowledge of site amplification) where there is none.

Note that while the centroid is described by a point location (the open star in Figure 5), its difference from the epicenter can portray source finiteness. For example, the centroid of the Northridge earthquake is well northwest (13 km) of the epicenter, and hence any predictive use of the centroid includes this northwestward shift.

INSTRUMENTAL SEISMIC INTENSITY MAPS

In addition to the PGA, PGV, and spectral response maps, we also map estimates of the ground-motion shaking intensity. Seismic intensity has been traditionally used worldwide as a method for quantifying the shaking pattern and the extent of damage for earthquakes. Though derived prior to the advent of today's modern seismometric instrumentation, seismic intensity still provides a useful means of describing information contained in these recordings. Such simplification is helpful for those users who are unfamiliar with instrumental ground motion parameters.

That is not to say that instrumentally derived seismic intensity alone is sufficient for loss estimation. In fact, peak velocity and spectral response may provide a more physical basis for such analyses. However, for the majority of users, we expect that the intensity map will be more readily interpreted than other maps of ground motion parameters.

Wald et al. (1999a) have recently developed regression relationships between Modified Mercalli intensity I_{mm} (Wood and Neumann, 1931, later revised by Richter, 1958), and PGA or PGV by comparing the peak ground motions to observed intensities for eight significant California earthquakes. For the limited range of Modified Mercalli intensities V $\leq I_{mm} \leq$ VIII, Wald et al. (1999a) found that for PGA,

$$I_{mm} = 3.66\ log(PGA) - 1.66 \quad (\sigma = 1.08) \tag{1}$$

and for peak velocity (PGV) within the range V $\leq I_{mm} \leq$ IX,

$$I_{mm} = 3.47\ log(PGV) + 2.35 \quad (\sigma = 0.98) \tag{2}$$

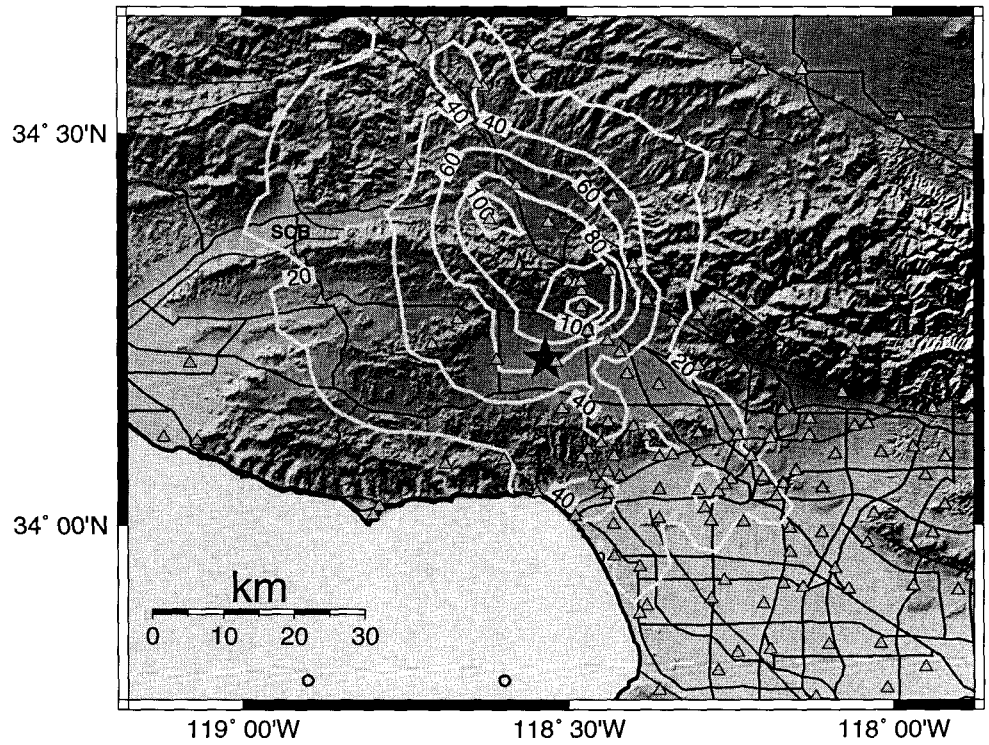

Figure 5. Shaded relief map showing recorded peak velocities, corrected for site amplification, for the magnitude 6.7 1994 Northridge earthquake. Velocity are units of cm/sec. The shaded star shows the epicenter, the open star represents the strong motion centroid, and open circles represent phantom grid stations. The location of the Santa Clara River Basin is shown with the letters "SCB."

Since we are also interested in estimating intensity at lower values, and our current collection of data from historical earthquakes does not provide constraints for lower intensity, we have imposed the following relationship between PGA and I_{mm}:

$$I_{mm} = 2.20\ log(PGA) + 1.00 \tag{3}$$

This basis for the above relationship comes from correlation of TriNet peak ground motions for recent magnitude 3.5 to 5.0 earthquakes with intensities derived from voluntary response from Internet users (Wald et al., 1999b) for the same events. We determined that the boundary between "not felt" and "felt" (I_{mm} I and II, respectively) regions corresponds to approximately one to two cm/sec/sec, at least for this range of magnitudes. We then assigned the slope such that the curve would intersect the relationship in Equation 1 at I_{mm} V. We plan to refine this relationship as more digital data become available. The corresponding equation for PGV and I_{mm} is:

$$I_{mm} = 2.10\ log(PGV) + 3.40 \tag{4}$$

By comparing maps of instrumental intensities with I_{mm} for eight significant Cal-

ifornia earthquakes (see Wald et al., 1999a), we have found that a relationship that follows acceleration for I_{mm}<VII and follows velocity for I_{mm}>VII works fairly well in reproducing the observed I_{mm}. In practice, we compute the I_{mm} from the I_{mm} verses PGA relationship (equations 1 and 3), and if the intensity value determined from peak acceleration is $\geq$ VII, we then use the value of I_{mm} derived from the I_{mm} verses PGV relationship (equation 2). If the I_{mm} determined from PGA is between V and VII, we weight both the PGA and PGV derived-values, ramping from a factor of 1.0 for PGA at I_{mm} V to 0.0 at I_{mm} VII.

Using peak acceleration to estimate low intensities is intuitively consistent with the notion that lower (<VI) intensities are assigned based on felt accounts, and people are more sensitive to ground acceleration than velocity. Higher intensities are defined by the level of damage; the onset of damage at the intensity VI to VII range is usually characterized by brittle-type failures (masonry walls, chimneys, unreinforced masonry, etc.) which are sensitive to higher-frequency accelerations. With more substantial damage (VII and greater), failure begins in more flexible structures, for which peak velocity is more indicative of failure (e.g., Hall et al., 1995). This practice is consistent with the recent analysis of Sokolov and Chernov (1998) in which they showed that seismic intensities correlate well for rather narrow ranges of Fourier amplitude spectra of ground acceleration, with 0.7-1.0 Hz being most representative of I_{mm} > VIII, while the 3-6 Hz range best represents I_{mm} V to VII, and the 7-8 Hz range best correlates with the lowest I_{mm} range. In addition, Boatwright et al. (1999) have found that for the Northridge earthquake, PGV and the 3-0.3 Hz averaged spectral velocity are better correlated with intensity (VI and greater) than peak acceleration and their correlation with intensity and peak spectral velocity is strongest at 0.67 Hz.

The legend below Figure 6 gives the peak ground motions that correspond to each unit Modified Mercalli intensity value according to our regression of the observed peak ground motions and intensities for California earthquakes. By relating recorded ground motions to Modified Mercalli intensities, we can now generate instrumental intensities within a few minutes of the event based on the recorded peak motions made at strong motion stations that will correspond approximately to the existing I_{mm} scale. In assigning integer intensity values using Equations 1-4, the rounding adheres to the convention that, for example, values between 5.50 and 6.49 round to intensity VI. Note that the estimated intensity map is derived from ground motions recorded by accelerographs and represents intensities that are likely to have been associated with the ground motions. However, unlike conventional intensities, the instrumental intensities are not based on observations of the earthquake effects on people or structures. Further, the range of peak values for a given intensity is likely to change as additional data sets are included.

Figure 6 shows the instrumental intensity map derived using the procedure outlined here using strong motion data recorded during the Northridge earthquake. The epicenter is shown with a solid star and blue lines depict highways. The color shading corresponds to the colored intensity scale shown below the figure, and two-word descriptions of both shaking and damage levels are provided (L. Dengler and J. Dewey, written communication, 1998). Given the current TriNet station distribution, we can recover most details of the Northridge intensity map (Figure 6), which is based on more densely spaced stations, if the CDMG dialup data are included (1/2 hour).

Figure 7 shows a comparison of the instrumental intensity contour lines and the

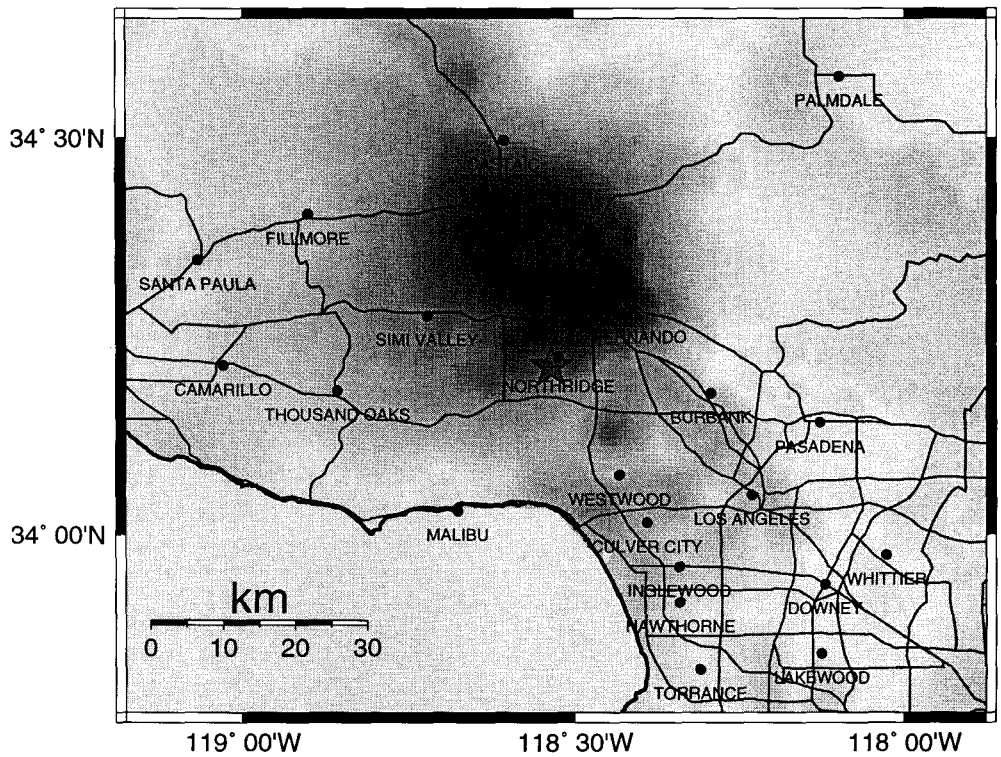

PERCEIVED SHAKING	Not felt	Weak	Light	Moderate	Strong	Very strong	Severe	Violent	Extreme
POTENTIAL DAMAGE	none	none	none	Very light	Light	Moderate	Moderate/Heavy	Heavy	Very Heavy
PEAK ACC.(%g)	*<.17*	*.17-1.4*	*1.4-3.9*	*3.9-9.2*	*9.2-18*	18-34	34-65	65-124	>124
PEAK VEL. (cm/s)	<0.1	0.1-1.1	1.1-3.4	3.4-8.1	8.1-16	*16-31*	*31-60*	*60-116*	*>116*
INSTRUMENTAL INTENSITY	I	II-III	IV	V	VI	VII	VIII		

Figure 6. Instrumental intensity map for the 1994 Northridge earthquake derived using the procedure outlined in the text. The epicenter is shown with a filled star; blue lines depict highways. The scale bar gives corresponding peak ground motion values and one- or two-word damage and perceived shaking descriptors.

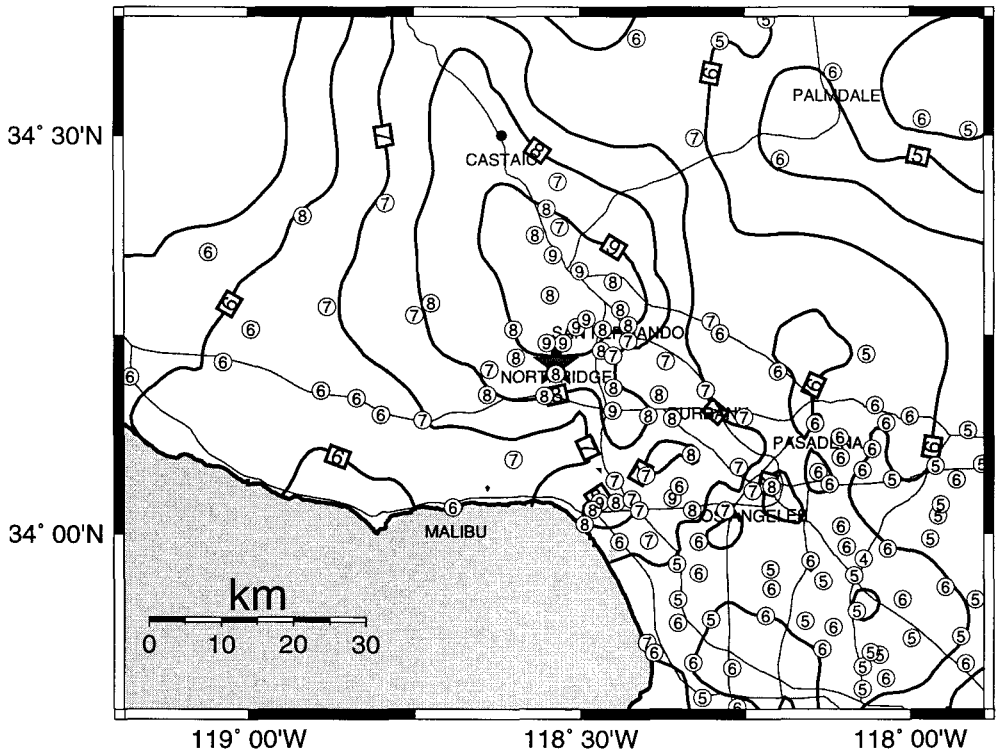

Figure 7. Instrumental intensity map for the 1994 Northridge earthquake derived using the procedure outlined in the text. Contour lines (thick lines) depict instrumental intensity values. Numbered circles give the observed Modified Mercalli intensity values of Dewey et al. (1995) for comparison. The epicenter is shown with a filled star; thin lines depict highways.

values of Modified Mercalli intensity observed by Dewey et al. (1995). The instrumental intensity map shares most of the notable features of the Modified Mercalli map prepared by Dewey et al. (1995), including the relatively high intensities near Santa Monica and southeast of the epicenter near Sherman Oaks. However, in general, the area of I_{mm} IX on the instrumentally derived intensity map is slightly larger than on the Dewey et al. (1995) map. This likely reflects the fact that although much of the Santa Susanna mountains, north and northwest of the epicenter, were very strongly shaken, the region is also sparsely populated, hence, observed intensities were not determined there. This is a fundamental difference between observed and instrumentally derived intensities: Instrumental intensities will show high levels of strong shaking, independent of the exposure of populations and buildings; observed intensities only represent intensities where there are structures to damage and people to experience the earthquake.

Though there is some degradation when the five-minute map is made using only the USGS-Caltech real-time stations, it nonetheless provides for more information than was available in the early morning of January 17, 1994. In that case it took over one half hour to provide just the epicenter and magnitude. Had this map been available in the minutes following the Northridge earthquake, much more would have been understood about the scope of the disaster and the variations in damage over the Los Angeles metropolis.

THE SHAKEMAP WEB PAGE

After triggering, events are automatically added to the database and are made available through the World Wide Web online interface. The Web site provides access to not only maps of the most recent earthquakes (for instance, a mainshock and significant aftershocks), but also events in the past processed to provide a basis for comparison with recent events. Once triggered, the actual processing of the peak acceleration, peak velocity, and intensity maps (including printing and complete Web page generation) takes less than one minute for the uncorrected maps; site corrections take an additional minute.

The Web maps are interactive. Selection of individual stations on the map initializes a lookup table that provides station information, including station names, coordinates, and the peak ground motion values recorded on each component. The web interface thus provides a convenient format for obtaining detailed strong motion information concerning specific sites. Such information has been long sought following major earthquakes, and now it can be provided in a rapid fashion.

For significant events (e.g., magnitude greater than 5.0), full-color, poster-sized maps are also generated automatically. In addition, a first motion mechanism (e.g., Reasenberg and Oppenheimer, 1975) and rapid moment tensor solution (Thio and Kanamori, 1995), are automatically added to the ShakeMap Web page. Summary files are also generated for each data set to be used for distribution. These files include the raw data, interpolated and site-corrected grid files and the values of the contour lines used on the maps.

DISCUSSION

Initially, our use of PGA and PGV for estimating intensities was simply practical. We were only retrieving peak values from a large subset of the network, so it was impractical to compute more specific ground-motion parameters, such as average response spectral values, kinetic energy, cumulative absolute velocities (CAV, EPRI, 1991), or the JMA intensity algorithm (Japan Meteorological Agency, 1996). However, since near-source ground motions are often dominated by short-duration pulses (usually associated with source directivity), PGV appears to be a robust measure of intensity for strong shaking. In other words, the kinetic energy available for damage is well characterized by PGV. The close correspondence of the JMA intensities and peak ground velocity (Kanezashi and Kaneko, 1997) indicates that our use of peak ground velocities for higher intensities is consistent with the algorithm used by JMA. Another consideration in the choice of peak ground motion values, rather than derived parameters, is the ease of relating intensity directly to simple ground motion observables.

For large distant earthquakes, the peak values will be less informative, and duration and spectral content may become key parameters. While we may eventually adopt corrections for these situations, it is difficult to assign intensities in such cases. For instance, what is the intensity in the zone of Mexico City where numerous high-rises collapsed during the 1985 Michoacan earthquake? It was obviously high intensity shaking for high rise buildings. However, the majority of smaller buildings were unaffected, indicating much lower intensity. While the peak ground velocities were moderate and would imply I_{mm} VIII, resonance and duration conspired to cause a more substantial disaster. Although this is, in part, a shortcoming of using peak parameters alone, it is more a limitation imposed by simplifying the complexity of ground motions into a single parameter.

Therefore, in addition to providing peak ground motion values and intensities, we are also producing spectral response maps (for 0.3, 1.0, and 3.0 sec), and those users who can take advantage of this information for loss estimation will have a clearer picture than can be provided with maps of PGA and PGV alone. However, as discussed earlier, a simple intensity map is extremely useful for the overwhelming majority of users, which includes the general public and many involved with the initial emergency response.

The use of PGV for higher intensities also proves important for several cases for which we have recorded a large, single-spike of high-frequency acceleration recorded for small earthquakes. With our procedure, while the large acceleration peak would provide an abnormally high intensity, the much smaller velocity amplitude provides a more appropriate, lower intensity. In contrast small earthquakes, which are nonetheless widely felt in many areas of southern California, generally provide noisy velocity recordings and hence the estimation of intensity from them alone is less reliable. For smaller events, acceleration amplitudes provide more reliable intensity estimates, though there are currently few data constraining the lowest intensity levels.

Our current scheme to include site amplification is admittedly crude. However, these simple geological classifications are attainable over the whole of southern California. A more detailed geological-based map for the region is being developed (M. Peterson, personal communication, 1998), and it will be incorporated into our system when it becomes available and can be tested. A compilation of more localized (and better constrained) site corrections based on either shallow soil velocity profiles or mainshock/aftershock studies (e.g., Hartzell et al., 1998) may improve the interpolation technique that we currently use. However, such data are not uniformly available and a new technique would have to be developed to incorporate such subsets into the interpolation scheme. Further, the effects of soil nonlinearity are not quantified in such site response maps since a majority of the ground motions were recorded at low levels of input motion, and these nonlinear effects could be important at the strong motion levels for which we anticipate ShakeMap will be most useful.

One implication of using site-corrections that depend on both frequency and amplitude (Table 1), is that the site corrections are smaller as amplitudes increase into the nonlinear range. Arguably, this range is for peak accelerations above about 20% g (e.g, Beresnev and Wen, 1996; Field et al., 1997). Hence, for intensity VII or greater, the site corrections (which are based on the peak velocity, or 1 Hz, correction factors) are relatively small.

It will also be important to delineate both the boundaries of potentially damaging near-source strong motions and also those regions at greater distances from the source, where there may be large site amplification. The frequency and amplitude dependence of site amplification on local site geology (average shear velocity) is still a rapidly evolving area of study. Fortunately, modifications to the amplification factors given in Table 1 can easily be implemented as more data and analyses become available.

We have not yet addressed the potential for severe site effects and liquefaction of soft soil in southern California (NEHRP categories E and F) such as in the Los Angeles Harbor region and along former and current river channels. Not only are we limited by the lack of sufficiently detailed geologic maps of such areas, but the connection between the surface geology and the site amplification is not fully established for strong motions.

Similarly, basin edge effects are not included, and differences between very deep basin and shallow basin sites are not yet distinguished. In addition, only peak values have been considered here; site resonance is not yet considered. Shaking duration has also not yet been included, though it may be important under certain circumstances. For instance, currently, we would likely underestimate the extent of damage (intensity) in Los Angeles for a great San Andreas event since only peak amplitude is considered. But currently there is little empirical constraint upon which to base a modification to the instrumental intensity computation for such an event. For such an earthquake, evaluation of the response spectral map may give more reliable estimates of potential damage.

The peak ground motion versus intensity correlation is based on observations collected from recent California earthquakes. Hence, this relationship is subject to revision to accommodate additional observations. At present, there is little data to correlate lower intensity values and recorded ground motions since most of the ground motion data are for larger earthquakes, and intensity data are not typically collected for smaller events. In addition, the calibration we have is primarily for analog recordings, so the noise level is high, especially for low amplitude (once-integrated) velocity seismograms. The digital data now being collected with TriNet will be more useful in calibrating against intensity at lower amplitudes. TriNet will provide low amplitude ground motion recordings, previously unavailable (or undigitized) with triggered, analog stations. We are also collecting intensity measurements at near-station locations through voluntary response on the Internet (Wald et al., 1999b) (URL *http://www-socal.wr.usgs.gov/ciim.html*). The combination of assigning intensities for low shaking levels with digital recordings will help constrain the relationship between acceleration and intensity at the lowest values.

Naturally, we are most concerned about accurately portraying the highest intensities. For example, approximately 86% of the residential losses in the Northridge earthquake occurred in the intensity VII-IX region (Kircher et al., 1997, p. 714). Intensity IX was the largest mapped value for that event. Interestingly, though, while the main emphasis of "ShakeMap" is to provide information about shaking for damaging earthquakes where the pattern of shaking can be quite complex, there has been widespread interest in viewing maps for smaller earthquakes which are, nonetheless, widely felt. We generate "ShakeMap" for all earthquakes in southern California above magnitude 3.0, but we only update the Web pages for magnitude 3.9 and greater, since the felt area for the smaller events is usually nominal. However, for several notable earthquakes in the magnitude 3.0 to 3.9 range, there has been a substantial demand for rapid display of the shaking pattern and so we have provided maps for these events as well. The advantage in providing ShakeMap for non-damaging earthquakes is twofold. First, we gain experience processing, calibrating, and checking our system by responding to small events daily to weekly, rather than on the very infrequent basis allowed by the occurrence of moderate to large earthquakes. Second, the user groups (which include emergency response agencies, utilities, the media, scientists, and the general public) are afforded the opportunity to become familiar with the maps and to test their response on a more regular basis.

CONCLUSIONS

Rapid estimation of shaking over the entire southern California region is accomplished by spatially interpolating ground motions recorded by TriNet using frequency and amplitude-dependent site corrections based on surface geology. Ground motions in areas of sparse station coverage are inferred from the data by using the centroid for forward estimation. As the real-time TriNet station density increases, the importance of the centroid for gap-filling will diminish, but currently it is imperative for the robust generation of ground motion maps. Fortunately, as planned, TriNet stations are more concentrated in heavily populated regions, so the most reliable recovery of the shaking distribution should be where potential losses and the need for concerted emergency response efforts could be the greatest. Newly developed relationships between recorded ground-motion parameters and expected shaking intensity (Wald et al., 1999a) allow us to also produce an instrumentally derived intensity map. This additional map allows us to rapidly portray the extent of shaking in a simplified form suitable for immediate post-earthquake decision-making. We have found that a relationship that follows acceleration for I_{mm}<VII and follows velocity for I_{mm}>VII works fairly well in reproducing the observed I_{mm} for a number of moderate to large earthquakes which have occurred in southern California.

One of the most important advances in loss estimation in recent years has been the development of methods such as HAZUS (Kircher et al., 1997; NIBS, 1997) that directly use instrumental ground motion observations in place of I_{mm}. ShakeMap will provide a much clearer picture of the nature and extent of ground motion following the next significant southern California earthquake and will provide a sound starting point for immediate loss estimation using such methods.

A critical component in successfully generating "ShakeMap" is a system that is robust; that is, it must function under the adverse conditions present during a damaging earthquake including strong shaking of computer equipment, power failures, communication problems, Internet bottlenecks, etc. Efforts have been ongoing to address these concerns. The World Wide Web uniform resource locator for the "ShakeMap" is *http://www.trinet.org/shake.html*

ACKNOWLEDGMENTS

Conversations with K. Campbell, R. Nigbor, and M. Petersen were very helpful. S. Park provided his QTM geology maps in digital form. Reviews by K. Campbell, M. Trifunac, R. Graves, and N. Field improved this manuscript, as did recommendations of Editorial Board Member P. Somerville. All the participants in TriNet played a critical role in this work, most notably D. Given, E. Hauksson, P. Maechling, and A. Shakal. Maps were made with Generic Mapping Tools (GMT, Wessel and Smith, 1991). Seismological Laboratory Contribution Number 8582. TriNet is funded by the OES/FEMA Hazard Mitigation Grant Program, Grant No. FEMA-1008-DR-CA, HMGP NO.003, FIPS No.037-90027; the USGS, the CDMG, the Calif. Trade and Commerce Agency, the Calif. Techology Investment Partnership Program; and private sector contributions.

REFERENCES CITED

Beresnev, I. A. and Wen, K.-L., 1996, Nonlinear soil response - a reality? (A review), *Bull. Seism. Soc. Am.*, **86**, 1964-1978.

Boatwright, J., Thywissen, K., and Seekins, L., 1999, Correlation of ground motion and intensity for the January 17, 1994, Northridge, California earthquake, submitted to *Bull. Seism. Soc. Am.*.

Boore, D. M., Joyner, W. B., and Fumal, T. E., 1994, Estimation of response spectra and peak accelerations from western North America earthquakes: An interim report, Part 2, *U.S. Geological Survey Open-File Report* **94-127**, 40 pp.

Borcherdt, R. D., 1994, Estimates of site-dependent response spectra for design (methodology and justification), *Earthquake Spectra*, **10**, 617-654.

Dewey, J. W., Reagor, B. G., Dengler, L., and Moley, K., 1995, Intensity distribution and isoseismal maps for the Northridge, California, earthquake of January 17, 1994, *U. S. Geological Survey Open-File Report* **95-92**, 35 pp.

Eguchi, R. T., Goltz, J. D., Seligson, H. A., Flores, P. J., Heaton, T. H., and Bortugno, E., 1997, Real-time loss estimation as an emergency response decision support system: The Early Post-Earthquake Damage Assessment Tool (EPEDAT), *Earthquake Spectra*, **13**, 815-832.

EPRI, 1991, Standardization of cumulative absolute velocity, EPRI TR100082 (Tier 1), Palo Alto, California, Electric Power Research Institute, Yankee Atomic Electric Company.

Field, E. H., Johnson, P. A., Beresnev, I. A., and Zheng, Y., 1997, Nonlinear sediment amplification during the 1994 Northridge earthquake, *Nature*, **390**, 599-602.

Hall, J. F., Heaton, T. H., Halling, M. W., and Wald, D. J., 1995, Near-source ground motions and its effects on flexible buildings, *Earthquake Spectra*, **11**, 569-606.

Hartzell, S. H., Harmsen, S., Frankel, A., Carver, D., Cranswick, E., Meremonte, M., and Michael J., 1998, First-generation site response maps for the Los Angeles region based on earthquake ground motions, *Bull. Seism. Soc. Am.*, **88**, 463-472.

Japan Meteorological Agency, 1996, Note on the JMA seismic intensity, JMA report 1996, *Gyosei* (in Japanese).

Joyner, W. B. and Boore, D. M., 1981, Peak horizontal accelerations and velocity from strong-motion records including records from the 1979 Imperial Valley, California, earthquake, *Bull. Seism. Soc. Am.*, **71**, 2011-2038.

Kanamori, H., 1993, Locating earthquakes with amplitude: Application to real-time seismology, *Bull. Seism. Soc. Am.*, **83**, 264-268.

Kanezashi, S. and Kaneko, F., 1997, Relations between JMA's measuring seismic intensity (MI) and phyical parameters of earthquake ground motion, *OYO Technical Report, 1997*, 85-96.

Kircher, C. A., Reitherman, R. K., Whitman, R. V., and Arnold, C., 1997, Estimation of earthquake losses to buildings, *Earthquake Spectra*, **13**, 703-720.

Mori, J., Kanamori, H., Davis, J., Hauksson, E., Clayton, R., Heaton, H., Jones, L., and Shakal, A., 1998, Major improvements in progress for southern California earthquake monitoring, *Eos Trans. AGU*, **79**, 217, 221.

National Institute of Building Sciences (NIBS), 1997, *Earthquake Loss Estimation Methodology: HAZUS97 Technical Manual*, Report prepared for the Federal Emergency Management Agency, Washington, D.C.

Park, S. and Ellrick, S., 1998, Predictions of shear wave velocities in southern California using surface geology, *Bull. Seism. Soc. Am.*, **88**, 677-685.

Reasenberg, P. and Oppenheimer, D., 1975, FPFIT, FPPLOT, and FPPAGE: Fortran programs for calculating and displaying earthquake fault plane solutions, *U. S. Geological Survey Open-File Report* **75-739**, 109 pp.

Shakal, A., Peterson, C., Cramlet, A., and Darragh, R., 1996, Near-real-time CSMIP strong motion monitoring and reporting for guiding event response, in *Proceedings of the 11th World Conference on Earth. Eng.*, Acapulco, Mexico.

Shakal, A., Peterson, C., and Grazier, V., 1998, Near-real-time strong motion data recovery and automated processing for post-earthquake utilization, *Proceedings of the Sixth U.S. Nat'l. Conference on Earth. Eng.*, Seattle.

Smith, W.H.F. and Wessel, P., 1990, Gridding with continuous curvature splines in tension, *Geophysics*, **55**, 293-305.

Sokolov, V. Y. and Chernov, Y. K., 1998, On the correlation of seismic intensity with Fourier amplitude spectra, *Earthquake Spectra*, **14**, 679-694.

Thio, H. K. and Kanamori, H., 1995, Moment tensor inversion for local earthquakes using surface waves recorded at TERRAscope, *Bull. Seism. Soc. Am.*, **85**, 1021-1038.

Wald, D. J., Heaton, T. H., Kanamori, H., Maechling, P., and Quitoriano, V., 1997, Research and development of TriNet "Shake" maps, *Eos Trans. AGU*, **78**, No. 46, p F45.

Wald, D. J., Quitoriano, V., Heaton, T. H., and Kanamori, H., 1999a, Relationships between peak ground acceleration, peak ground velocity and Modified Mercalli Intensity in California, *Earthquake Spectra*, **15**, 557-564.

Wald, D. J., Quitoriano, V., Dengler, L., and Dewey, J. W., 1999b, Utilization of the Internet for rapid community seismic intensity maps, *Seism. Res. Lett.*, in press.

Wessel, P. and Smith, W.H.F., 1991, Free software helps map and display data, *Eos Trans. AGU*, **72**, 444-446.

Wood, H. O. and Neumann, F., 1931, Modified Mercalli Intensity scale of 1931, *Bull. Seism. Soc. Am.*, **21**, 277-283.

Yamakawa, K., 1998, The Prime Minister and the earthquake: Emergency management leadership of Prime Minister Marayama on the occasion of the Great Hanshin-Awaji earthquake disaster, *Kansai Univ. Rev. Law and Politics*, **19**, 13-55.